Supplementary Information (SI) for RSC Advances.

This journal is © The Royal Society of Chemistry 2025

Supporting Information for

Metal–Organic Framework–Injectable Hydrogel Hybrid Scaffolds Promote Accelerated Angiogenesis for In Vivo Tissue Engineering

Sobuj Shahidul Islam, Tatsuya Dode, Soma Kawashima, Myu Fukuoka, Takaaki Tsuruoka,* and Koji Nagahama*

Department of Nanobiochemistry, Frontiers of Innovative Research in Science and Technology (FIRST), Konan University, 7-1-20 Minatojima-minamimachi, Chuo-ku, Kobe 650-0047, Japan.

*Corresponding author.

K. Nagahama. Tel: +81-78-303-1328; E-mail: nagahama@konan-u.ac.jp

T. Tsuruoka. Tel: +81-78-303-1452; E-mail: tsuruoka@konan-u.ac.jp

(A)

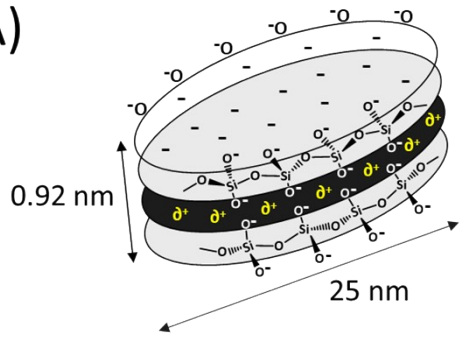

LAPONITE

$Na^{+0.7}[(Si_8Mg_{5.5}Li_{0.3})O_{20}(OH)_4]^{-0.7}$

(B)

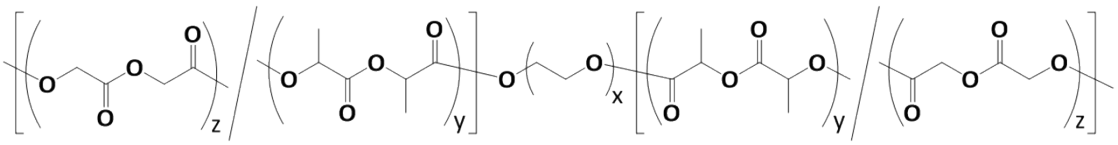

poly(lactide-*co*-glycolide)-*b*-poly(ethylene glycol)-*b*-poly(lactide-*co*-glycolide)
(PLGA-PEG-PLGA)

Fig. S1. Structures of (A) LAPONITE and (B) PLGA-PEG-PLGA copolymer.

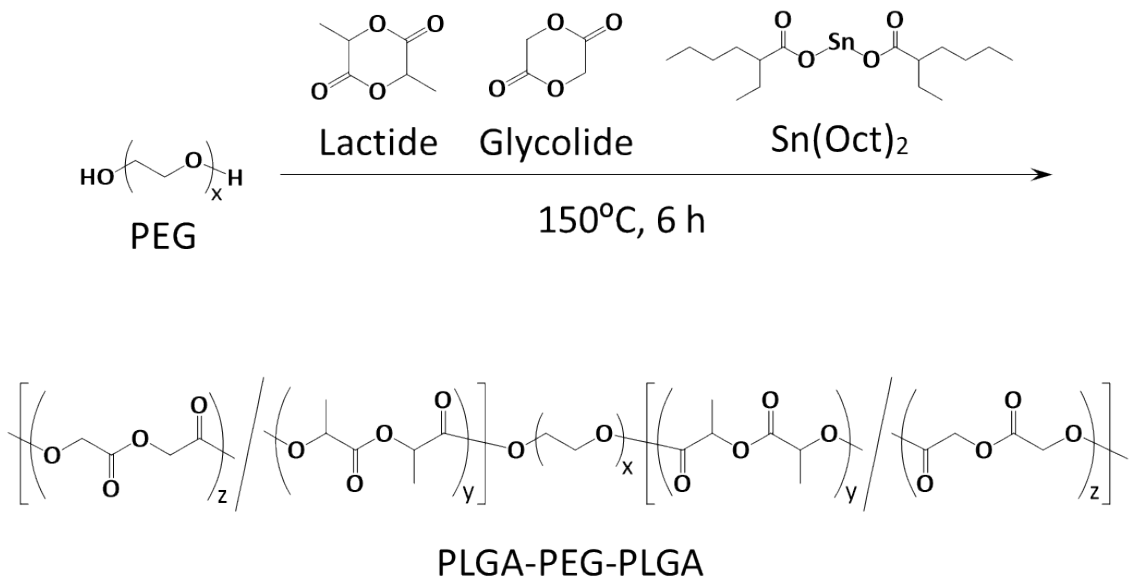

Scheme S1. Synthesis of PLGA-PEG-PLGA copolymer.

Table S1. Characterization of the synthesized PLGA-PEG-PLGA copolymers.

DP of LA [a]	DP of GA [a]	M_w of PEG	M_w of copolymer [b]	M_w/M_n [c]
8	4	3,000	6,300	1.27

[a] Estimated by ^{1}H-NMR.

[b] Estimated by the following equation: M_w of copolymer = M_w of PEG segment + 2 × (M_w of PLGA segment).

[c] Estimated by GPC (eluent: DMSO, standard: PEG).

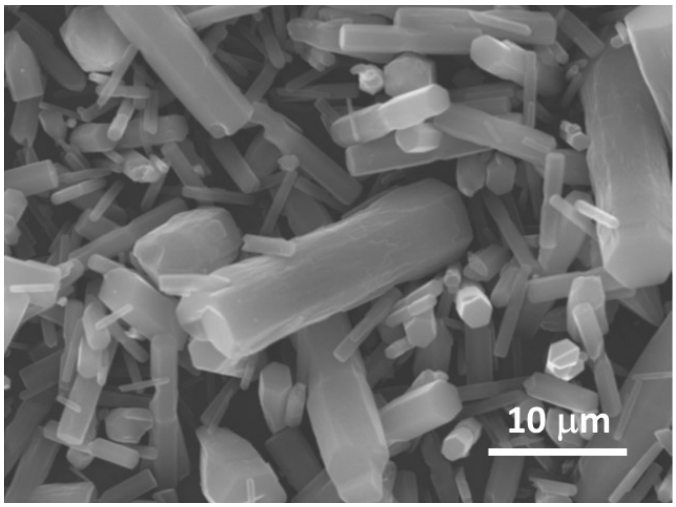

Fig. S2. SEM image of the synthesized NU-1000.

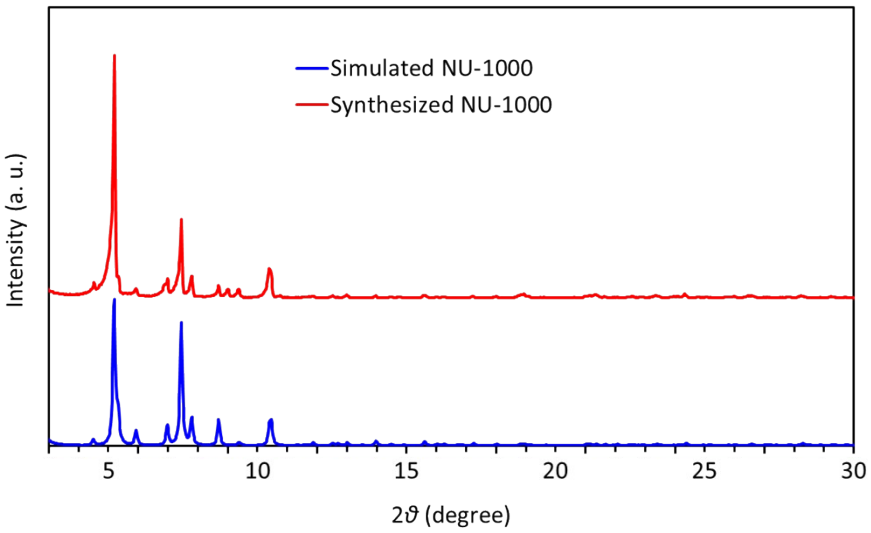

Fig. S3. Wide-angle X-ray diffraction pattern of the synthesized NU-1000.

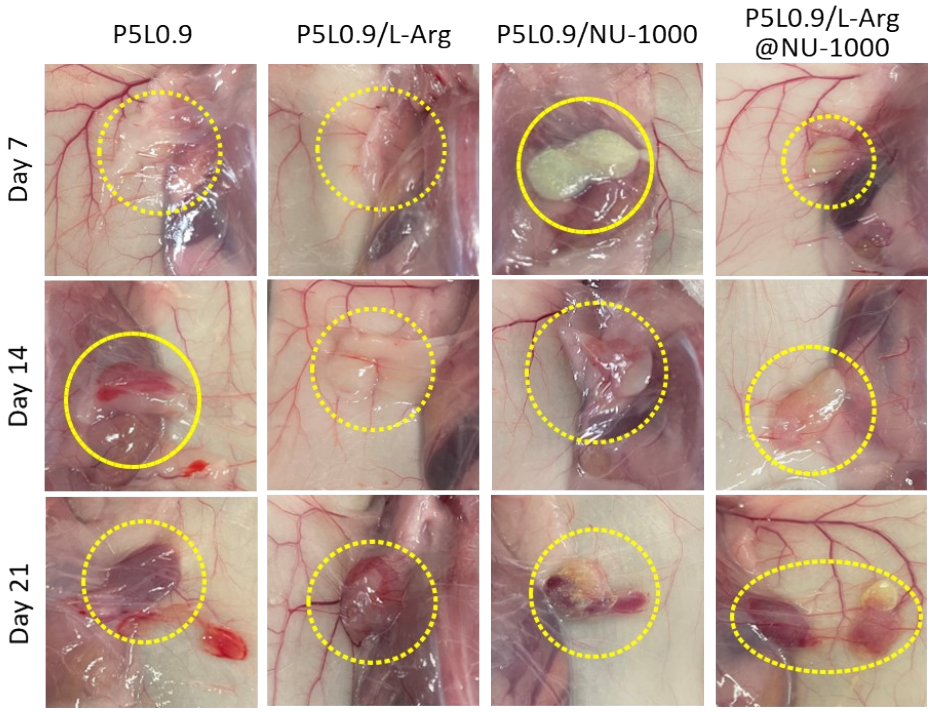

Fig. S4. Representative images of the hydrogels with surrounding tissue at 7, 14, and 21 days after administration of P5L0.9 hydrogels, L-arginine-loaded P5L0.9 hydrogels, NU-1000-composited P5L0.9 hydrogels, and L-arginine-loaded NU-1000-hybrid P5L0.9 hydrogels.

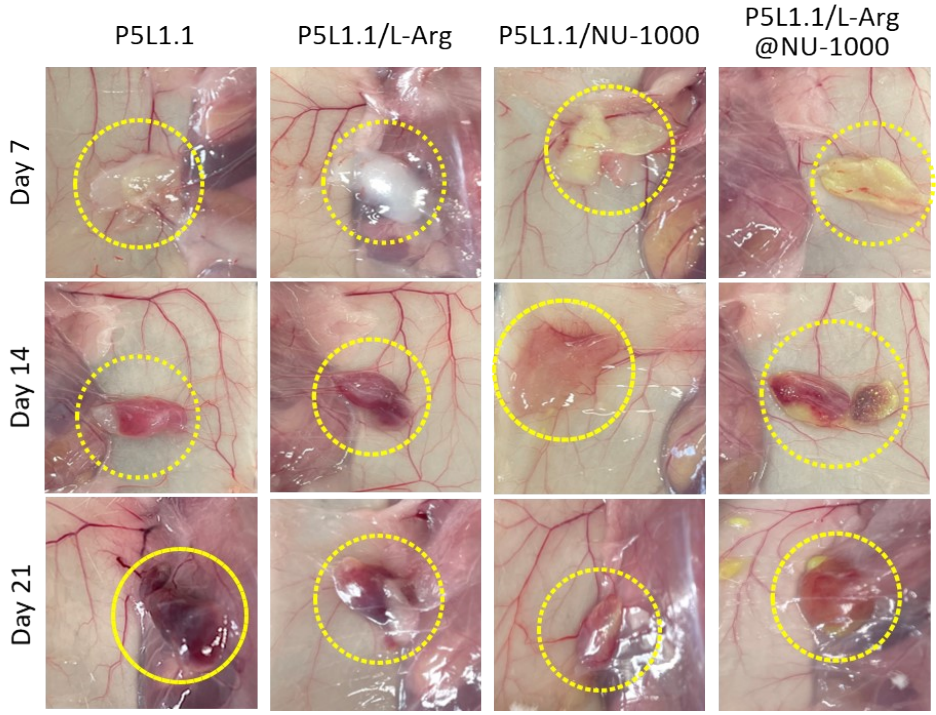

Fig. S5. Representative images of the hydrogels with surrounding tissue at 7, 14, and 21 days after administration of P5L1.1 hydrogels, L-arginine-loaded P5L1.1 hydrogels, NU-1000-composited P5L1.1 hydrogels, and L-arginine-loaded NU-1000-hybrid P5L1.1 hydrogels.

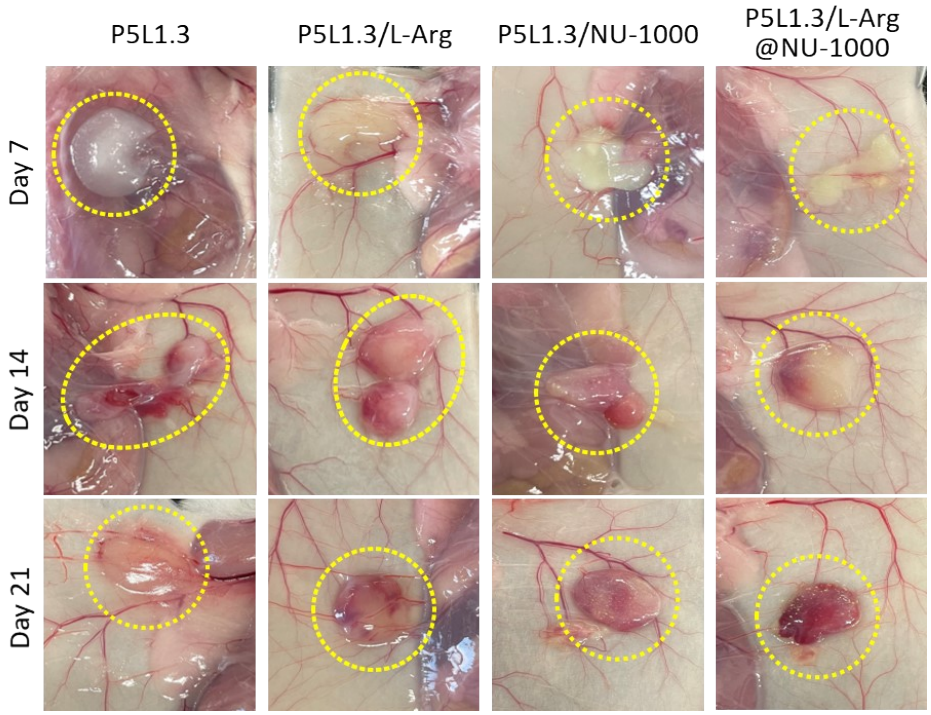

Fig. S6. Representative images of the hydrogels with surrounding tissue at 7, 14, and 21 days after administration of P5L1.3 hydrogels, L-arginine-loaded P5L1.3 hydrogels, NU-1000-composited P5L1.3 hydrogels, and L-arginine-loaded NU-1000-hybrid P5L1.3 hydrogels.

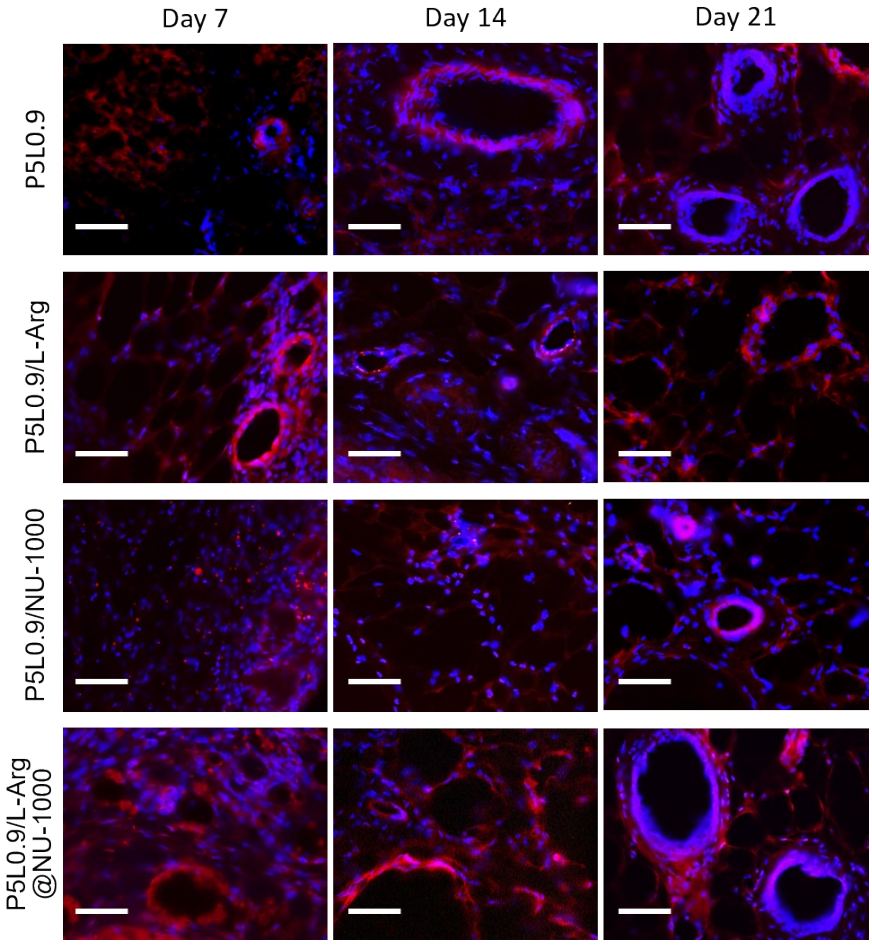

Fig. S7. Representative fluorescence microscopic images of the hydrogels formed in the subcutaneous tissue of mice. At days 7, 14, and 21 after administration of P5L0.9 hydrogels, L-arginine-loaded P5L0.9 hydrogels, NU-1000-composited P5L0.9 hydrogels, and L-arginine-loaded NU-1000-hybrid P5L0.9 hydrogels, these hydrogels were carefully removed from the mice and immunofluorescence staining for CD31 was performed. Blue: DAPI and red: CD31 (Alexa Fluor®567).

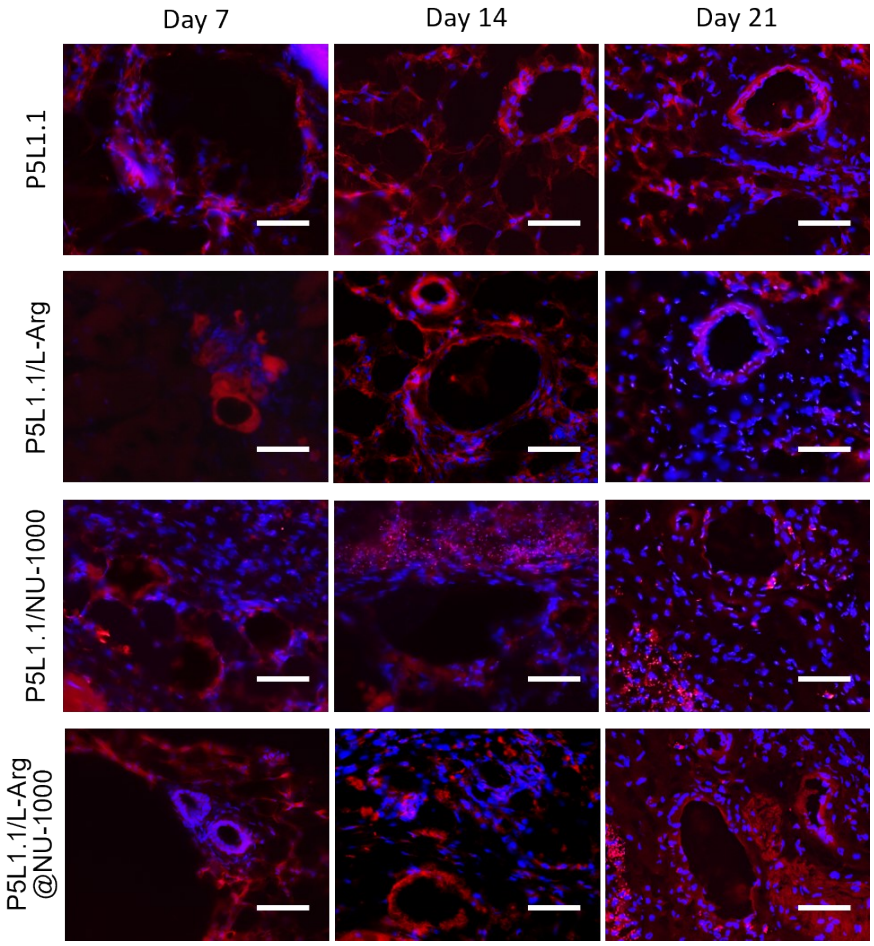

Fig. S8. Representative fluorescence microscopic images of the hydrogels formed in the subcutaneous tissue of mice. At days 7, 14, and 21 after administration of P5L1.1 hydrogels, L-arginine-loaded P5L1.1 hydrogels, NU-1000-composited P5L1.1 hydrogels, and L-arginine-loaded NU-1000-hybrid P5L1.1 hydrogels, these hydrogels were carefully removed from the mice and immunofluorescence staining for CD31 was performed. Blue: DAPI and red: CD31 (Alexa Fluor®567).

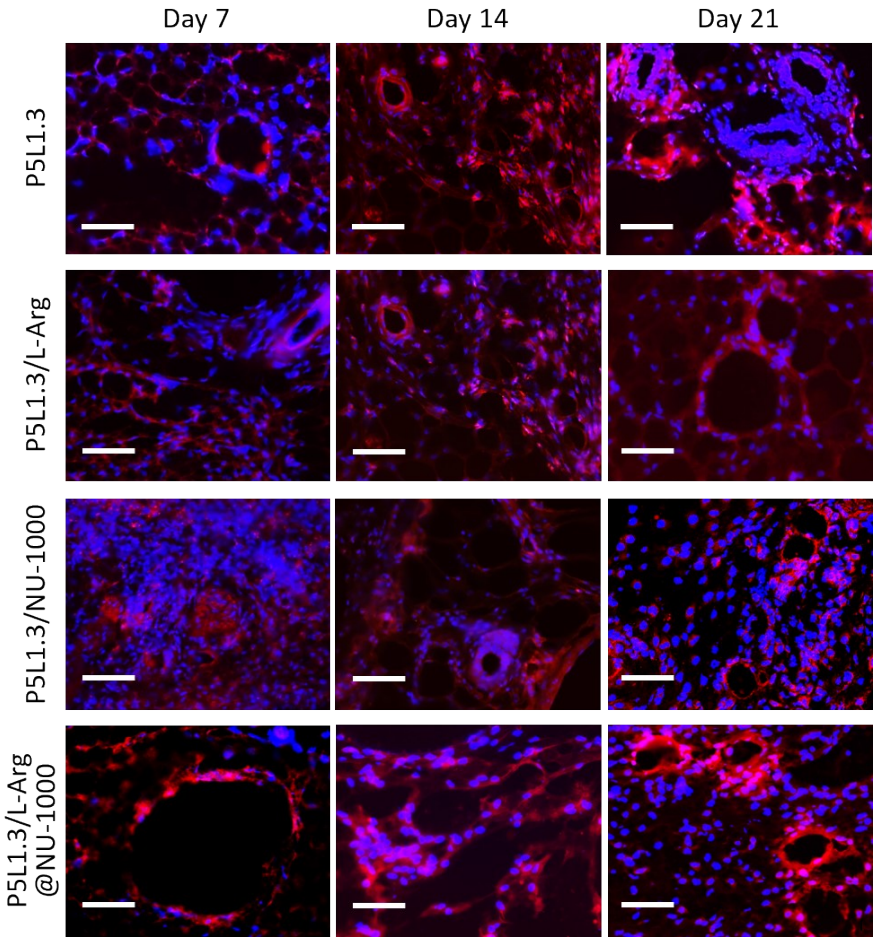

Fig. S9. Representative fluorescence microscopic images of the hydrogels formed in the subcutaneous tissue of mice. At days 7, 14, and 21 after administration of P5L1.3 hydrogels, L-arginine-loaded P5L1.3 hydrogels, NU-1000-composited P5L1.3 hydrogels, and L-arginine-loaded NU-1000-hybrid P5L1.3 hydrogels, these hydrogels were carefully removed from the mice and immunofluorescence staining for CD31 was performed. Blue: DAPI and red: CD31 (Alexa Fluor®567).